

# **EARTHQUAKE HAZARD IN PACIFIC NORTHWEST: RUPTURE AREA OF GREAT EARTHQUAKES AND ORIGIN OF PUGET SOUND CRUSTAL SEISMICITY**

R.D. Hyndman, H. Dragert, K. Wang, S. Mazzotti

Pacific Geoscience Centre  
9860 W. Saanich Rd., Sidney B.C. V8L 4B2, Canada  
and School of Earth and Ocean Sciences, University of Victoria  
tel: (250) 363-628, fax: (250) 363-6565, email: hyndman@pgc.nrcan.gc.ca

April 2002 Final report: USGS NEHRP External Grant 01HQGR0004

NEHRP Element I and II, Pacific Northwest; Keywords: Seismotectonics, GPS-continuous, Neotectonics, Paleoseismicity

*Research supported by the U.S. Geological Survey (USGS), Department of the Interior, under USGS award number (Hyndman et al., 01HQGR0004). The views and conclusions contained in this document are those of the authors and should not be interpreted as necessarily representing the official policies, either expressed or implied, of the U.S. Government.*

## **ABSTRACT**

This grant was to support earthquake hazard studies in the Pacific Northwest. We report results regarding the distributions and rates of two major earthquake sources based on the deformation rates measured by GPS and other geodetic data, and determined from other geological data. These results provide: 1) Better constraints on the seismogenic portion of the Cascadia subduction megathrust and on strain accumulation along that fault; and 2) From geodetic and geological data, constraints on the recurrence rates of large crustal earthquakes in the Cascadia forearc, as well as potential for large characteristic events that are not predicted by the catalogue statistics of smaller earthquakes.

## **RESULTS**

### **1. Constraints on the rupture area of the Cascadia great earthquakes**

Constraints on the rupture zone (and strain accumulation) of the Cascadia subduction megathrust have been derived from GPS and other geodetic measurements along the Cascadia forearc. These data constrain numerical models for the portion of the subduction megathrust that is locked and may rupture in great earthquakes.

#### ***1.1. Megathrust transient versus forearc long-term deformation***

Along the Cascadia subduction zone part of the forearc is migrating to the north parallel to the margin. As a consequence, GPS measurements in the forearc are affected by two process: 1) Transient strain accumulation due to coupling of the locked subduction thrust; 2) Long-term geological motion and deformation of the forearc.

Accurate estimation of the strain accumulation due to the megathrust locked zone and definition of the width of the locked zone depends on separating those two components.

This separation has been done by correcting the measured GPS velocities (with respect to North America) using the predicted displacement field associated with the forearc northerly motion and long-term crustal deformation. Because the two processes (subduction coupling and forearc deformation) are inter-related on the few year time-scale of GPS measurements, the modeling of both processes was done iteratively. Advances in the understanding of each system were used to improve the model for the other. The separation of the two signals is facilitated because the elastic strain accumulation on the megathrust dominates the GPS signal in the outer forearc, whereas the forearc motion and ongoing deformation dominate the inner forearc.

To constrain the extent of the megathrust locked and transition zones, the GPS data were corrected for a model of forearc long-term motion and deformation as described in section 2.1. This forearc motion model is constrained by geodetic, paleomagnetic and geological data.

### ***1.2. Vancouver Island and northern Washington velocity and strain rate fields***

GPS velocity data in southwestern British Columbia and northwestern Washington have been derived from a permanent network of continuous stations (Western Canada Deformation Array) and from three campaign networks that cover most of Vancouver Island and adjacent Washington. Campaign data were acquired and processed as part of a PGC / University of Victoria PhD thesis (Henton et al., 1999, 2000).

The main results from analysis of the crustal velocity field constrained by these

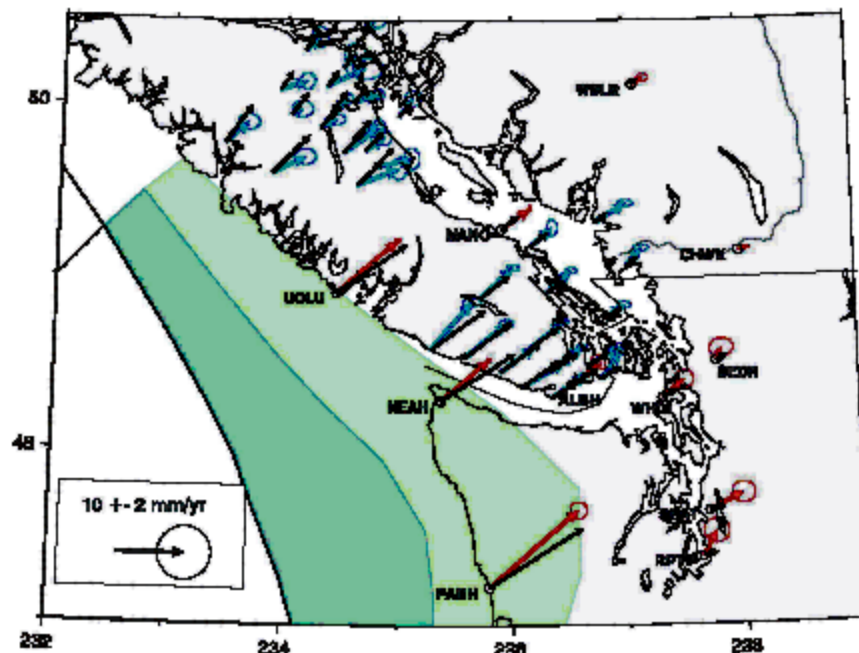


**Figure 1:** GPS velocities in northern Cascadia. Red, blue and black vectors are continuous GPS, campaign GPS, and predicted velocities, respectively. Dark and light green areas are model locked and transition zones of the Cascadia megathrust.

GPS data are summarized below (Henton et al., 1999, 2000):

1) To a first order, the GPS velocities and strain rates indicate the Cascadia subduction thrust is fully locked as far north as the Nootka fault zone off central Vancouver Island (Figure 1).

2) The data distribution in northern Vancouver Island is not good enough, as yet, to constrain whether the Explorer segment has a locked subduction fault.

3) Measurements in central Vancouver Island do not show significant strain rate accumulation in the region of the M ~7, 1918 and 1946 crustal earthquakes. Thus, the recurrence rate of this type of events must be low.

4) The misfit between the GPS data and a simple 3D elastic strain accumulation model is associated to a slower landward decrease of the GPS velocities, compared to the predicted loading velocities. This conclusion lead us to investigate the possibility of more complex time-dependent model of the subduction zone (c.f., section 1.4).

### ***1.3. Formal inversion for subduction fault coupling***

Most previous constraints for the locked and transition zone on the subduction thrust have come from forward modelling. As part of this study, continuous and campaign GPS velocities were used to constrain a formal inversion of the subduction thrust coupling rate off central and southern Vancouver Island (Yoshioka et al., 2001).

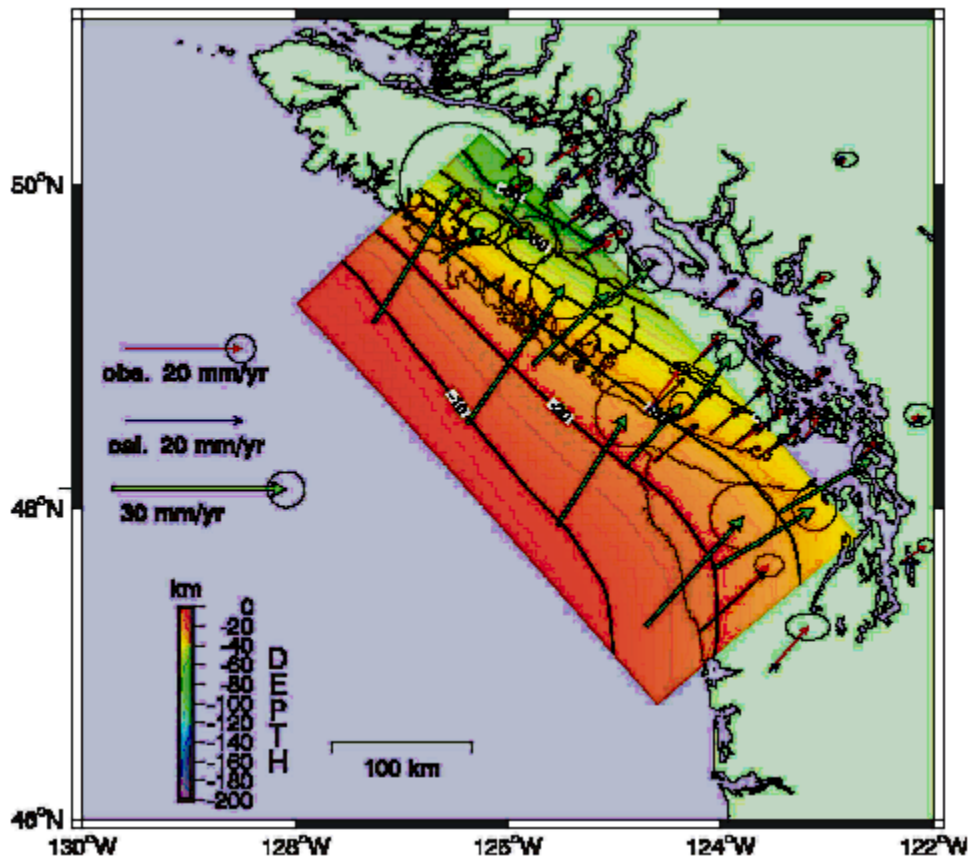


**Figure 2:** Inversion for interseismic locking of the northern Cascadia megathrust. Red, blue and green arrows represent the measured GPS, predicted, and interseismic slip deficit velocities, respectively.

The inversion was based on method previously used along the Nankai trough and the Japan trench. This approach indicated a strongly locked zone and a downdip transition zone very similar to those used in the forward modeling (Figure 2). The inversion results also highlight the need for a large transition zone to fit the slow landward decay of the GPS velocity field.

#### ***1.4. Revised elastic and time-dependent modeling of interseismic deformation***

Most previous models for the strain field associated with a locked subduction thrust assume constant strain accumulation through the interseismic period. As part of this work, the misfit between the GPS velocity data and the simple elastic strain accumulation model (section 1.2) was addressed by a new model that allows for the temporal behavior of the subduction zone after a great megathrust earthquake (Wang et al., 2002). The new elastic dislocation model includes a larger transition zone (compared to the standard model) with a downdip exponential increase of the steady interseismic slip (from zero to full free slip), and a transition zone that changes with time. The model introduced the concept of "effective transition zone" to mimic the visco-elastic behavior of the subduction fault and upper mantle. The fit to the GPS velocities and strain rates was significantly improved, especially for the more landward sites.

Based on this model, a megathrust earthquake scenario was developed, assuming 500 years of slip deficit (~18 m), a coseismic rupture that takes place at full slip over the entire locked zone, and slip decreasing to zero half way down the present-day transition zone. Thus, the coseismic rupture landward extent is less than the extent of the current locked and transition zones. The predicted coseismic deformation pattern is in general agreement with the 1700 earthquake coastal subsidence and tsunami data.

## **2. Recurrence rate and location of $M > 7$ crustal earthquakes: Seattle-Portland area hazard**

A strong concentration of crustal earthquakes occurs in the Portland-Seattle-Vancouver region (Figure 4). Because these earthquakes occur at shallow depth in the Cascadia forearc they represent a large seismic hazard for the Puget Lowland and the Georgia Basin region of S.W. British Columbia. Good constraints on the maximum magnitude and recurrence rates of these earthquakes are critical inputs to the seismic hazard assessment for this region. In particular, in this study, we addressed whether the available earthquake statistics, based mainly on small magnitude events, provide a reliable constraint for the frequency of large earthquakes. Especially, can large "characteristic earthquakes" be expected in the Puget Sound - Georgia basin area?

This question was approached through estimating the rate of large earthquakes required to accommodate observed crustal deformation rates. Our method is to compare the crustal deformation rates derived from catalogue earthquake statistics with that from geodetic and geological data. If the rate from the latter is greater, large infrequent events may occur that are not predicted by the catalogue statistics. An extreme example of characteristic earthquakes is the Cascadia megathrust that has few if any small events, only  $M \sim 9$  earthquakes. Another example may be the area of central Vancouver Island where two  $M \sim 7$  earthquakes occurred in 1918 and 1946, and where there is very little current seismicity.

## 2.1. Estimates of N-S shortening from GPS and geological data

Focal mechanism solutions for crustal earthquakes in the Puget Lowland - SW British Columbia region indicate that the main compressive stress is horizontal N-S (margin-parallel). The crustal deformation rate of the forearc associated with this tectonic regime was estimated as part of this study using permanent and campaign GPS data along the Cascadia forearc (Mazzotti et al., 2002; see also Khazaradze et al., 1999).

GPS velocity vectors from four different analysis (WCDA, Dragert et al., 1995; PANGA, Miller et al., 2001, Oregon campaign, McCaffrey et al., 2000; Vancouver Island campaign, Henton et al., 2000) were formally combined into a common solution referenced to GPS station DRAO (Penticton, BC, Canada), well inland of the deforming forearc. GPS derived strain rates indicate that most of the Cascadia forearc undergoes an uniaxial margin-normal shortening associated with the subduction transient strain, except for the northwestern Washington region, where significant N-S shortening is evidenced.

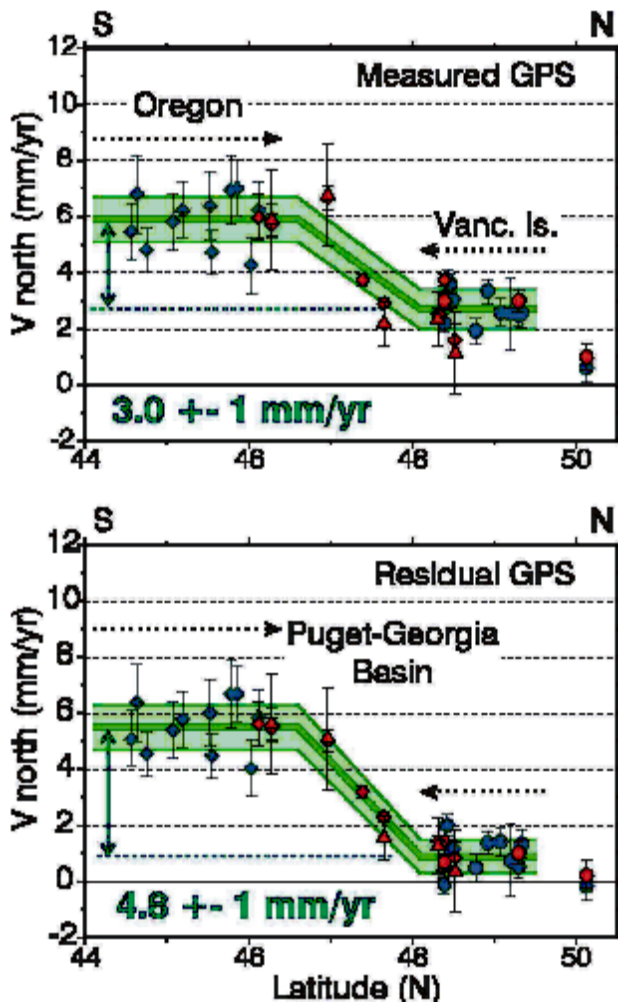


**Figure 3:** Puget Lowland - South Georgia Basin shortening rate measured by GPS. (a) Top: North component of current GPS velocities versus latitude. (b) Bottom: Long-term northward GPS velocities (current GPS corrected for transient subduction interseismic loading). Red and blue symbols are continuous and campaign data, respectively.

A plot of the GPS northward velocity versus latitude shows that the present-day N-S shortening is concentrated between 46.5 and 48 °N and reaches  $3.0 \pm 0.7$  mm/yr in the Puget Sound - South Georgia Basin area (Figure 3a).

As mentioned previously, GPS data are affected by both long-term geological deformation of the forearc and transient strain accumulation along the subduction fault. The long-term shortening of the forearc was estimated by removing from the GPS data the predicted northerly component of velocities due to the current locking of the subduction thrust. The model used to predict the interseismic subduction loading effect was constrained by recent estimations of the plate convergence, forearc motion, and locked zone extent (c.f., Section 1).

The long-term N-S shortening in the Puget Sound - South Georgia Basin region (longer than great earthquake cycle) was estimated to be  $4.8 \pm 0.6$  mm/yr (Figure 3b).

This value is slightly less but within the uncertainties of estimated N-S convergence between the Oregon forearc and southwestern British Columbia based on geological data and tectonic models, including:

1) Fault slip rate estimates along the major crustal faults in the northern Cascadia forearc (e.g., Seattle fault) that indicate a total convergence of  $\sim 4$  mm/yr in western Washington (e.g., Wells and Simpson, 2000).

2) Block models of the relative Oregon forearc / North America motion indicate a northward velocity of the Oregon block of 6-7 mm/yr at  $\sim 46^\circ\text{N}$  (e.g., Wells et al., 1998, McCaffrey et al., 2000).

The difference between the GPS and these estimates suggest that some  $\sim 1$  mm/yr shortening may be accommodated to the north and south of the main zone of shortening.

## ***2.2. Crustal earthquake statistics***

In order to derive forearc deformation rates from crustal earthquakes, an initial review and integration of the available catalogues has been carried out, and the properties of these events investigated (e.g., location, depth, frequency, etc.; see Hyndman et al., 2002).

### **2.2.a. Location and depth distribution**

Small to medium magnitude crustal forearc earthquakes along the Cascadia margin concentrate in the Puget Lowland - South Georgia Basin region (Figure 4). This is where most active crustal faults have been mapped. Seismicity becomes insignificant eastward along the Cascade volcanic arc and westward in the Olympic Mountains. We note that the only three large ( $M > 7$ ) historical earthquakes recorded in the Cascadia forearc are located outside of this region of high seismic activity (Figure 4). These events could be characteristic earthquakes (i.e., associated with little background seismicity). This pattern raises the questions of whether such characteristic earthquakes can occur in the Puget Lowland region, and whether the small magnitude earthquake statistics can be used to reliably estimate large event recurrence rates.

The depth distribution of crustal events is well constrained. An E-W cross section indicates that most of the earthquakes lie within a 12-15 km thick layer. This layer is located between 10 and 25 km depth below the Seattle basin in the Puget Sound area (Figure 5). The lack of seismicity in the upper 10 km may be due to aseismically deforming Tertiary sedimentary basins. The earthquakes rise to 0-15 km eastward, toward the volcanic arc, presumably because of the eastward heat flow increase and shallowing of the thermally limited base of seismicity as the arc is approached.

### **2.2.b Active faults, paleo-earthquakes, and maximum magnitude**

Four main active faults have been recognized in the Puget Lowland - South Georgia Basin region: the Tacoma, Seattle, South Whidby Island, and Devil Mountain faults. The best studied motion is a large paleo-earthquake ( $M \sim 7.3$ ) that was evidenced along the Seattle fault about 900 AD (e.g., Bucknam et al., 1992). An empirical relationship between fault size and earthquake magnitude (Wells and Coppersmith, 1994) suggests a maximum magnitude  $M = 7.5$ , if the Seattle ruptured entirely along a 150 km long section.

### **2.2.c Magnitude-frequency distribution**

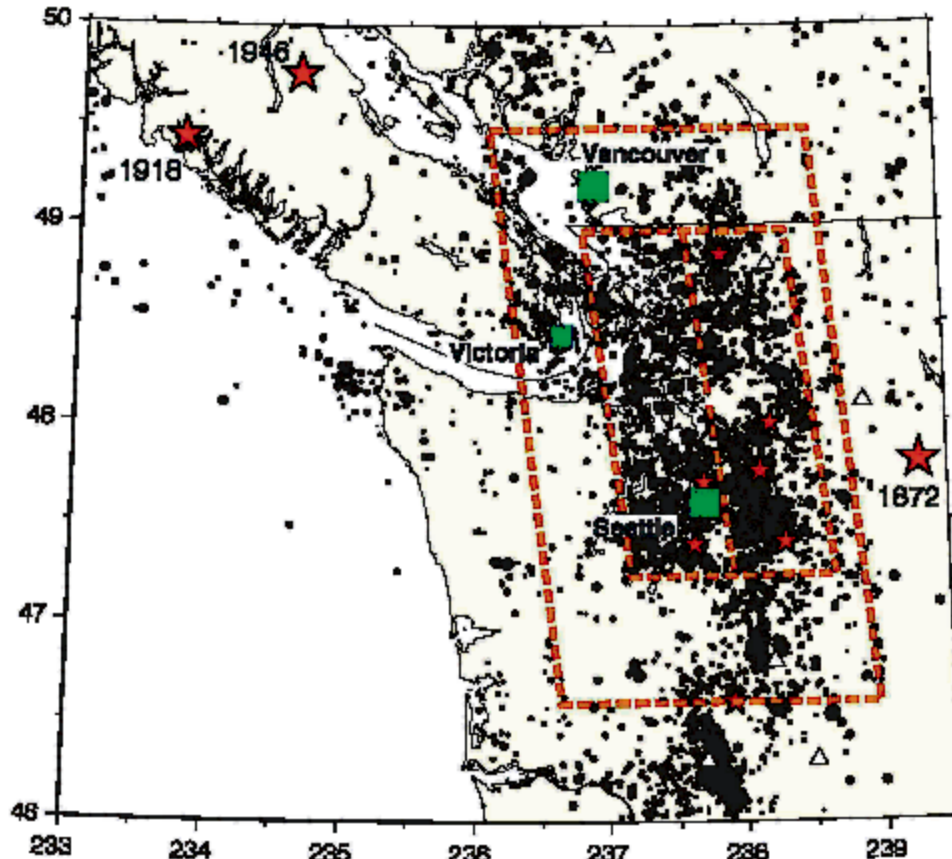


**Figure 4:** Crustal earthquakes in western Washington and southwestern British Columbia. Black circles are  $M > 2$  shallow (depth  $< 30$  km) earthquakes for 1980-2000. Red stars are medium to large ( $M > 5$ ) crustal earthquakes since 1872. Orange dashed boxes show zones used for earthquake statistics.

The magnitude-frequency (Gutenberg-Richter) distribution of crustal earthquakes in the Puget Lowland - South Georgia Basin region was estimated using a catalogue of events of magnitude  $M > 2$ , from 1900 to 1999. The data come from merging Geological Survey of Canada (GSC), University of Washington (UW), and U.S. Geological Survey (USGS) catalogues. For the Puget Sound region, UW event locations were combined with  $M_L$  magnitudes from the GSC, since the UW magnitudes are mainly coda or duration which have a less well calibrated relation to seismic moment. The cumulative recurrence relation is given by:

$$\log(N) = a - bM$$

where  $N$  is the cumulative number of earthquake of magnitude  $M$  and above, and  $a$  and  $b$  are the intercept and slope of the linear distribution.

The completeness of the catalogue varies with magnitude. Two approaches can be used to account for this effect: 1) Consider earthquake data limited to a time period for which all events above a specified magnitude are complete; 2) Derive statistics for time interval varying with earthquake magnitude. The formal treatment for the latter was developed by Weichert (1980). The statistics for both techniques were found to be consistent, but the recurrence is much better constrained using the latter method. The following results are base on the second approach with completeness periods as follow:

$M > 5.75$ , 1899;  $M > 5.25$ , 1917;  $M > 4.75$ , 1940;  $M > 3.75$ , 1956;  $M > 2.75$ , 1970;  $M > 2.45$ , 1976.

The stability of the magnitude-frequency distribution was checked by testing the sensitivity to the lower magnitude cut-off ( $M_0$ ) and to the earthquake distribution area. The statistics were found to be stable for the two different areas considered (large and small boxes, Figure 4), the  $b$  value ranging between 0.72 and 0.75 for  $M_0 = 3.5$  (Figure 6; Hyndman et al., 2002). Because the recurrence statistics are mostly constrained by small to mid magnitudes, they showed more sensitivity to the lower magnitude cut-off. The  $b$  values varied from 0.69 to 0.82 for  $M_0$  between 2.5 and 4.0.

Large crustal earthquakes recurrence rates, based on extrapolation of small and mid-size earthquakes for the large box of Figure 4, are 0.0209 /yr ( $\sim 1/50$  yr) for  $M > 6$  and 0.0024 /yr ( $\sim 1/420$  yr) for  $M > 7$  (Figure 6; Table 1; Hyndman et al., 2002).

### ***2.3. Large earthquake recurrence and crustal deformation rate***

#### **2.3.a From earthquake recurrence to deformation rate**

In order to constrain earthquake recurrence rates using measurements of crustal deformation rates, a four step process was used to related earthquake statistics to seismic moment and deformation:

##### **1) Magnitude-frequency distribution**

As described in the previous section, earthquake statistics for events of magnitude  $M > 3.5$  were used to constrain the parameters  $a$  and  $b$  of the magnitude-frequency distribution of crustal seismicity.

##### **2) Magnitude to moment**

Magnitude rates were converted to seismic moment rates using an empirical relationship developed by Hanks and Kanamori (1979) for local magnitude  $M_L$ :

$$\log (M_0) = 9.05 + 1.5 M_L$$

This relationship was used for successfully comparing earthquake moment rate to fault slip rate in California (e.g., Field et al., 1999). Initial work on comparing catalogue magnitudes with seismic moments from moment tensor solutions in the region (J. Ristau, personal communication 2002) give good agreement with this relation.

##### **3) Total moment**

Using the two previous steps, the total seismic moment rate  $M_o'$  was estimated by integrating the magnitude-frequency distribution up to a given maximum magnitude  $M_X$ :

$$M_o' = b 10^{(1.5 - b) MX + a + 9.05} / (1.5 - b)$$

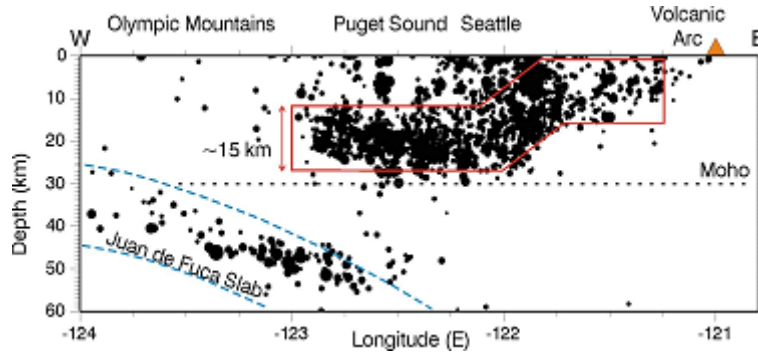


**Figure 5:** Cross section of crustal earthquakes in northwestern Washington. Black circles are  $M \geq 2$  earthquakes for 1980-2000 along 50 km wide cross section centered on  $47.5^\circ\text{N}$ .

The maximum magnitude was assumed to be  $M_x = 7.5 \pm 0.2$ . Because of the asymmetry of the stochastic moment-magnitude relation, a small correction of +27% was applied to the computed total moment rate to allow for statistical scatter (Hyndman and Weichert, 1983).

#### 4) Moment rate to deformation rate

The deformation rate associated with the crustal seismicity was estimated by assuming that: a) Deformation within a 250 km wide by 12 km thick region was fully seismic; b) Seismicity was mainly accommodated along E-W striking,  $45^\circ$  dipping, thrust faults; and c) Magnitude-frequency distribution and magnitude to moment relationship were similar for the entire magnitude range (i.e., no magnitude dependency). The total

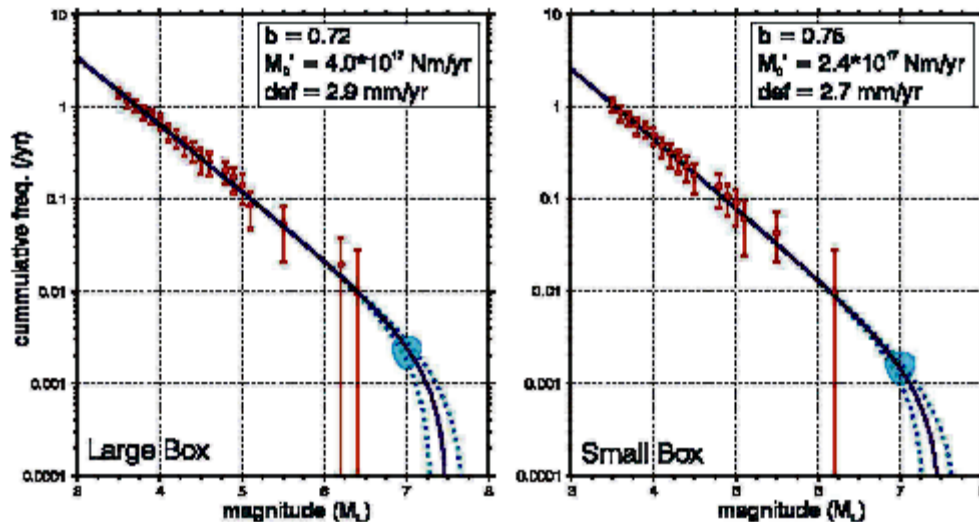


**Figure 6:** Frequency-magnitude distribution of crustal earthquakes in Puget Lowland - South Georgia Strait. Crustal (depth  $< 30$  km) earthquakes  $M \geq 3.5$ . Large (left) and small (right) regions correspond to boxes in Figure 4. Solid blue line shows the best-fit frequency-magnitude relationship for maximum magnitude  $M_x = 7.5$ . Dashed light blue lines show relationship for  $M_x = 7.3$  and  $M_x = 7.7$ .  $b$ : slope of frequency-magnitude distribution;  $M_0'$ : Total seismic moment rate; def: N-S shortening rate derived from earthquake statistics.

seismic N-S shortening rate  $d'$  derived from earthquake statistics was given by:

$$d' = \frac{1}{2} * M_0' / (\mu A)$$

where  $\mu = 3.3 * 10^{10}$  N/m<sup>2</sup> is the medium shear modulus, and  $A = 250 * 12$  km<sup>2</sup> is the seismic cross section area.

### **2.3.b Earthquake recurrence constrained by deformation rates**

The N-S shortening rate derived from crustal seismicity in the Puget Lowland - South Georgia Basin region is  $d' = 2.9 \pm 1.0$  mm/yr. The associated total seismic moment rate is  $M_0' = 4.0 * 10^{17}$  Nm/yr (Table 1; Hyndman et al., 2002).

This seismic deformation rate is in good agreement with GPS measurements that indicate present-day N-S shortening rate of  $3.0 \pm 0.7$  mm/yr (c.f., section 2.1). This rate represents a total seismic moment of  $M_0' = 4.1 * 10^{17}$  Nm/yr. The GPS-derived N-S shortening rate implies recurrence rates for crustal earthquakes 0.0025 /yr ( $\sim 1/390$  yr) for  $M \geq 7$ , in agreement with earthquake statistics within the uncertainties.

Long-term N-S shortening rate, as constrained by GPS and other geological data, is 4-6 mm/yr in the western Washington - southwestern British Columbia region. The long-term GPS rate ( $4.8 \pm 0.6$  mm/yr) represents a total seismic moment rate of  $M_0' = 6.7 * 10^{17}$  Nm/yr, which may be accommodated by a recurrence rate for  $M \geq 7$  earthquakes of 0.0034 yr ( $\sim 1/290$  yr), somewhat larger than predicted by earthquake statistics extrapolation but within the uncertainties.

**Table 1: Seismic deformation rates and large earthquake recurrence rates**

		<i>Shortening rate</i>	<i>Total moment rate</i>	<i>M &gt; 7 frequency</i>
		(mm/yr)	(10 <sup>17</sup> Nm/yr)	(/yr)
<i>Earthquake statistics</i>	$M_x=7.3$	$2.1 \pm 0.5$	$2.9 \pm 0.6$	$1/(590 \pm 70)$
	$M_x=7.5$	$2.9 \pm 0.6$	$4.0 \pm 0.8$	$1/(420 \pm 50)$
	$M_x=7.7$	$4.1 \pm 0.9$	$5.7 \pm 1.1$	$1/(345 \pm 50)$
	Mean	<b><math>2.9 \pm 1.0</math></b>	<b><math>4.0 \pm 1.4</math></b>	<b><math>1/(420 \pm 120)</math></b>
<i>GPS measurement</i>	Current	$3.0 \pm 0.7$	$4.1 \pm 1.0$	$\sim 1/(390 \pm 60)$
	Long-term	$4.8 \pm 0.6$	$6.7 \pm 0.8$	$\sim 1/(290 \pm 50)$

### **2.3.c Characteristic earthquakes**

The comparison of large crustal earthquake recurrence rates predicted by earthquake statistics and by GPS-derived crustal deformation indicates that characteristic earthquakes are not required to accommodate the measured shortening of the northern Cascadia forearc. Earthquake statistics are consistent, within the uncertainties, with both current and long-term estimates of N-S shortening rate in the Puget Lowland - South Georgia Basin. The predicted recurrence rate for  $M \geq 7$  crustal earthquakes is 1/400-1/300 yr.

Although not statistically significant, the difference between the recurrence rate derived from earthquake statistics ( $\sim 1/400$  yr) and that derived from long-term deformation rate ( $\sim 1/300$  yr) suggest that large crustal earthquakes may occur somewhat more often than suggested by the extrapolation small earthquake statistics. An

interesting possibility relates these 'extra' crustal events to the giant earthquakes along the Cascadia megathrust. The coseismic deformation during a subduction earthquake could induce up 0.5-1 m of abrupt N-S shortening in the western Washington forearc. This sudden N-S strain and stress increase could increase the probability for crustal earthquakes along Seattle fault-type structures for some time following the great event (Mazzotti et al., 2002).

## REFERENCES

- Buckman, R.C., Hemphill-Haley, E., and Leopold, E.B., Abrupt uplift within the past 1700 years at southern Puget Sound, Washington, *Science*, 258, 1611-1614, 1992.
- Dragert, H., Chen, X., and Kouba, J., GPS monitoring of crustal strain in southwest British Columbia with the Western Canadian Deformation Array, *Geomatica*, 49, 301-313, 1995.
- Field, E.H., Jackson, D.D., and Dolan, J.F., A mutually consistent seismic-hazard source model for southern California, *Bull. Seism. Soc. Amer.*, 89, 559-578, 1999.
- Hanks, T.C., and Kanamori, H., A moment magnitude scale, *J. Geophys. Res.*, 84, 2348-2350, 1979.
- Henton, J.A., Dragert, H., Hyndman, R.D., and Wang, K., Geodetic monitoring of crustal deformation and strain on Vancouver Island, *EOS Trans. AGU*, 80, F276, 1999.
- Henton, J.A., Dragert, H., McCaffrey, R., Wang, K., and Hyndman, R.D., GPS monitoring of deformation at the northern Cascadia subduction zone, *EOS Trans. AGU*, 81, F328, 2000.
- Hyndman, R.D., and Weichert, D.H., Seismicity and rates of relative motion on the plate boundaries of western North America, *Geophys. J. Roy. Astron. Soc.*, 72, 59-82, 1983.
- Hyndman, R.D., Mazzotti, S., Weichert, D.H., and Rogers, G.C., Large earthquake rate of occurrence in Puget Sound-S. Georgia Strait predicted from geodetic and geological deformation rates, *J. Geophys. Res.*, *subm.*, 2002.
- Khazaradze, G., Qamar, A., and Dragert, H., Tectonic deformation in western Washington from continuous GPS measurements, *Geophys. Res. Lett.*, 26, 3153-3156, 1999.
- Mazzotti, S., Dragert, H., Hyndman, R.D., Miller, M.M., and Henton, J.A., GPS deformation in a region of high crustal seismicity: N. Cascadia forearc, *Earth Planet. Sci. Lett.*, 198, 41-48, 2002.
- McCaffrey, R., Johnson, C.K., Zwick, P.C., Long, M.D., Goldfinger, C., Nabelek, J.L., and Smith, C., Rotation and plate locking along the southern Cascadia subduction zone, *Geophys. Res. Lett.*, 21, 3117-3120, 2000.
- Miller, M.M., Johnson, D.J., Rubin, C.M., Dragert, H., Wang, K., Qamar, A., and Goldfinger, C., GPS determination of along-strike variations in Cascadia margin kinematics: Implications for relative plate motion, subduction zone coupling, and permanent deformation, *Tectonics*, 20, 161-176, 2001.
- Wang, K., Wells, R., Mazzotti, S., and Hyndman, R.D., A revised dislocation model of interseismic deformation of the Cascadia subduction zone, *J. Geophys. Res.*, *subm.*, 2002.

- Weichert, D.H., Estimation of the earthquake recurrence parameters from unequal observation periods for different magnitudes, *Bull. Seis. Soc. Am.*, 70, 1337-1346, 1980.
- Wells, D.L., and Coppersmith, K.J., New empirical relationships among magnitude, rupture length, rupture width, rupture area, and surface displacement, *Bull. Seism. Soc. Amer.*, 84, 974-1002, 1994.
- Wells, R.E., Weaver, C.S., and Blakely, R.J., Forearc migration in Cascadia and its neotectonics significance, *Geology*, 26, 759-762, 1998.
- Wells, R.E., and Simpson, R.W., Northward migration of the Cascadia forearc in the northwestern US and implications for subduction deformation, *PANGA Annual Meet.*, Corvallis (OR), 2000.
- Yoshioka, S., Wang, K., and Mazzotti, S., Locking state of the northern Cascadia megathrust fault inferred from inversion of GPS velocities, *EOS Trans. AGU*, 82, F278, 2001.

#### **Publications from this study:**

- Henton, J.A., GPS studies of crustal deformation in the northern Cascadia subduction zone, PhD Thesis, University of Victoria, 169pp, 2000.
- Henton, J.A., Dragert, H., Hyndman, R.D., and Wang, K., Geodetic monitoring of crustal deformation and strain on Vancouver Island, *EOS Trans. AGU*, 80, F276, 1999.
- Henton, J.A., Dragert, H., McCaffrey, R., Wang, K., and Hyndman, R.D., GPS monitoring of deformation at the northern Cascadia subduction zone, *EOS Trans. AGU*, 81, F328, 2000.
- Hyndman, R.D., Mazzotti, S., Weichert, D.H., and Rogers, G.C., Large earthquake rate of occurrence in Puget Sound-S. Georgia Strait predicted from geodetic and geological deformation rates, *J. Geophys. Res.*, subm., 2002.
- Mazzotti, S., Dragert, H., Hyndman, R.D., Miller, M.M., and Henton, J.A., GPS deformation in a region of high crustal seismicity: N. Cascadia forearc, *Earth Planet. Sci. Lett.*, 198, 41-48, 2002.
- Miller, M.M., Johnson, D.J., Rubin, C.M., Dragert, H., Wang, K., Qamar, A., and Goldfinger, C., GPS determination of along-strike variations in Cascadia margin kinematics: Implications for relative plate motion, subduction zone coupling, and permanent deformation, *Tectonics*, 20, 161-176, 2001.
- Wang, K., Wells, R., Mazzotti, S., and Hyndman, R.D., A revised dislocation model of interseismic deformation of the Cascadia subduction zone, *J. Geophys. Res.*, subm., 2002.
- Yoshioka, S., Wang, K., and Mazzotti, S., Locking state of the northern Cascadia megathrust fault inferred from inversion of GPS velocities, *EOS Trans. AGU*, 82, F278, 2001.